IEEE Access
Multidisciplinary | Rapid Review | Open Access Journal

Received August 1, 2018, accepted September 3, 2018, date of publication September 6, 2018,
date of current version September 28, 2018.

Digital Object Identifier 10.1109/ACCESS.2018.2868988

Continuous Nonsingular Fast Terminal Sliding Mode Control of Cable-Driven Manipulators With Super-Twisting Algorithm

YAOYAO WANG[1,2,3], (Member, IEEE), FEI YAN[1], JIAWANG CHEN[3], (Member, IEEE), AND BAI CHEN[1]

[1]College of Mechanical and Electrical Engineering, Nanjing University of Aeronautics and Astronautics, Nanjing 210016, China
[2]State Key Laboratory of Fluid Power and Mechatronic Systems, Zhejiang University, Hangzhou 310027, China
[3]Ocean College, Zhejiang University, Hangzhou 310029, China

Corresponding author: Yaoyao Wang (yywang_cmee@nuaa.edu.cn)

This work was supported in part by the National Natural Science Foundation of China under Grant 51705243, in part by the Natural Science Foundation of Jiangsu Province under Grant BK20170789, in part by the Open Foundation of the State Key Laboratory of Fluid Power and Mechatronic Systems under Grant GZKF-201606, and in part by the China Postdoctoral Science Foundation under Grant 2018M630552.

ABSTRACT For the high-accuracy tracking control purpose of cable-driven manipulators under complex lumped uncertainties, a novel continuous nonsingular fast terminal sliding mode (CNFTSM) control scheme using a modified super-twisting algorithm (STA) is proposed and investigated in this paper. The proposed method applies the time-delay estimation (TDE) technique to estimate and compensate the unknown lumped system dynamics leading to an attractive model-free nature. Then, the NFTSM manifold and the modified STA scheme are used to ensure finite-time convergence performance in both the reaching and sliding mode phases. Thanks to the TDE technique, the proposed method is model-free and suitable to use in complicated practical applications; meanwhile, fast convergence, high tracking accuracy, and good robustness against lumped uncertainties can be ensured befitting from the CNFTSM control with NFTSM error dynamics and STA schemes. Stability of the closed-loop control system is proved. Finally, 2 degrees of freedom comparative simulations and experiments were performed to demonstrate the effectiveness and superiorities of our proposed method over the existing TDE-based robust control schemes.

INDEX TERMS Continuous nonsingular fast terminal sliding mode, cable-driven manipulator, time-delay estimation, super-twisting algorithm.

I. INTRODUCTION

In the past few decades, robot manipulators had been widely used in both academic and industrial applications due to their good ability to realize accurate automatic work [1]–[4]. Usually, the drive units of traditional robot manipulators are directly installed in the joints to achieve fast dynamic response and high control accuracy. However, this kind of design will bring in large moving inertia, high stiffness and low flexibility, which is not safe for the physical interactions with human. Therefore, the cable-driven manipulators were proposed and investigated to effectively settle these problems [5], [6]. Different from traditional robot manipulators, the cable-driven ones enjoy small moving inertia, good flexibility and safe physical interactions with human by installing the drive units in/near the base instead of the joints [7]–[9]. Due to these obvious advantages, cable-driven manipulators are becoming a research hotspot [10]–[13].

However, the application of cable-driven technique has also brought in extra difficulties for controller designing, which mainly contains joint flexibility, relative low stiffness and complicated system dynamics. Therefore, it still remains a challenging task to design a suitable controller for the cable-driven manipulators. To effectively solve above mentioned problems, some robust controllers had been proposed and investigated for the system with flexibility, such as sliding mode (SM) control [14], neural network control [15], adaptive control [16] and iterative learning control [17]. The former, *i.e.* SM control, has attracted lots of attention benefitting from its strong robustness against uncertainties and essential simplicity to use [18]–[22]. The core idea of SM control is to design a proper manifold and then use a switching element to enforce the system trajectory to converge to the manifold and stay on it [23]. To successfully realize above process, the switching element has to be selected sufficiently large,

which, however, may result in chattering issue. The chattering issue is a well-known main disadvantage of SM control and will lead to obvious control performance degradation, large energy consumption and even damages to the hardware.

To effectively overcome the chattering for SM controls, several techniques had been utilized, such as boundary layer technique [18], continuous reaching law [24], adaptive methods [25], [26], intelligent methods [27], [28] and high-order SM (HOSM) controls [29], [30]. The latter has drawn much interest thanks to its strong capability to handle the chattering while still provide with satisfactory control performance. Several HOSM controls had been presented to achieve chattering suppression and high control performance [31], [32], while super-twisting algorithm (STA) is one of the most effective schemes [33]–[35]. STA can generate continuous control signal that enforces the SM manifold convergence to zero in finite time resulting in high control accuracy and good dynamic performance. Although good theoretical and experimental results had been obtained with above-mentioned methods, they may be not suitable for complex practical applications due to the requirement of system dynamics or complicated approximation algorithm.

Time-delay estimation (TDE) is a straightforward but effective way to conquer above issues. The main idea of TDE is to estimate the remaining lumped system dynamics using just the time delay states which will bring in a fascinating model-free nature [36], [37]. Thanks to this attractive model-free scheme, TDE had been widely used in lots of systems, such as robot manipulators [38]–[40], underwater vehicles [41], [42], exoskeleton robots [43], [44]. Since TDE uses only the time delay states to estimate the lumped system dynamics, corresponding estimation error, *i.e.* TDE error, will be inevitable especially when system experiences fast changes. To cope with TDE error and achieve high tracking accuracy, SM controls are usually adopted. Nevertheless, most existing TDE-based SM controls still use traditional ways to suppress the chattering, which in turn may limit the improvement of control performance. Recently, a novel TDE-based SM control was reported which uses STA to suppress the chattering and ensure good tracking control performance [45]. Although good theoretical and experimental results had been reported in [45], it can still be further improved. Traditional SM manifold with linear error dynamics was used, which can only guarantee asymptotic convergence of the control error. Moreover, standard STA scheme was applied which may lead to unsatisfactory control performance when the system trajectory is relative far away from the equilibrium point.

In this paper, aforementioned issues are properly handled. A novel TDE-based continuous nonsingular fast terminal SM (CNFTSM) control using modified STA scheme is proposed and investigated. The proposed method utilizes TDE technique to estimate the unknown remaining system dynamics and brings in an attractive model-free scheme; afterwards, the CNFTSM control with modified STA is utilized to achieve finite time convergence and high performance in both the reaching and sliding mode phases. The proposed method is model-free and easy to use in complicated practical applications due to TDE, and can guarantee satisfactory control performance thanks to the CNFTSM control with modified STA. Corresponding stability of the closedloop control system is given. Finally, the superiorities of the proposed method are demonstrated through comparative simulations and experiments.

The contributions of this paper are listed as:

1) to propose a novel TDE-based CNFTSM control using modified STA scheme. By combining an improved NFTSM manifold, a modified STA and the TDE technique, the newly proposed method can provide with better comprehensive control performance than the existing one from [45];
2) to prove the stability of the closed-loop control system with NFTSM and modified STA dynamics;
3) to demonstrate the superiorities of the newly proposed method by comparative simulations and experiments.

The remainder is given as follows. Section II briefly gives some preliminaries. Then, the proposed method is given and analyzed in Section III. Section IV presents the stability analysis, meanwhile Section V and VI gives the comparative simulation and experimental studies. Finally, Section VII concludes this paper.

II. PRELIMINARIES

A. DYNAMICS OF A CABLE-DRIVEN MANIPULATOR

The dynamics of a cable-driven manipulator with n-DOFs (degree of freedoms) can be described as [46]

$$\mathbf{J}\ddot{\boldsymbol{\theta}} + \mathbf{D}_m\dot{\boldsymbol{\theta}} = \boldsymbol{\tau}_m - \boldsymbol{\tau}_s \tag{1}$$

$$\mathbf{M}(\mathbf{q})\ddot{\mathbf{q}} + \mathbf{C}(\mathbf{q},\dot{\mathbf{q}})\dot{\mathbf{q}} + \mathbf{G}(\mathbf{q}) + \mathbf{Fr}(\mathbf{q},\dot{\mathbf{q}}) + \boldsymbol{\tau}_d = \boldsymbol{\tau}_s \tag{2}$$

$$\boldsymbol{\tau}_s = \mathbf{K}_s(\boldsymbol{\theta} - \mathbf{q}) + \mathbf{D}_s\left(\dot{\boldsymbol{\theta}} - \dot{\mathbf{q}}\right) \tag{3}$$

where $\boldsymbol{\theta}$, $\mathbf{q}$ stand for the motor/joint position. $\boldsymbol{\tau}_m$, $\boldsymbol{\tau}_s$ represent the drive torque generated by motors and joint compliance torque given in (3). $\mathbf{J}$ and $\mathbf{D}_\mathrm{m}$ stand for the motor iner-tia and damping matrices, $\mathbf{M}(\mathbf{q})$, $\mathbf{C}(\mathbf{q},\dot{\mathbf{q}})$, $\mathbf{G}(\mathbf{q})$, $\mathbf{Fr}(\mathbf{q},\dot{\mathbf{q}})$ are the inertia matrix, Coriolis/ centrifugal matrix, gravitational vector and friction vector, respectively. $\boldsymbol{\tau}_d$ stands for the lumped disturbance, while $\mathbf{K}_\mathrm{s}$ and $\mathbf{D}_\mathrm{s}$ are the joint stiffness and damping matrices.

Combining (1) and (2) and using a constant $\bar{\mathbf{M}}$ matrix yields

$$\bar{\mathbf{M}}\ddot{\mathbf{q}} + \mathbf{H} = \boldsymbol{\tau}_m \tag{4}$$

where $\bar{\mathbf{M}}$ is usually tuned by simulation or experimental studies. The element $\mathbf{H}$ stands for the remaining dynamics of the system, which can be mathematically defined as

$$\mathbf{H} \triangleq \underbrace{\left(\mathbf{M} - \bar{\mathbf{M}}\right)\ddot{\mathbf{q}} + \mathbf{C}(\mathbf{q},\dot{\mathbf{q}})\dot{\mathbf{q}} + \mathbf{G}(\mathbf{q}) + \mathbf{Fr}(\mathbf{q},\dot{\mathbf{q}})}_{\text{remainding manipulator dynamics}} + \underbrace{\mathbf{J}\ddot{\boldsymbol{\theta}} + \mathbf{D}_m\dot{\boldsymbol{\theta}}}_{\text{motor dynamics}} + \underbrace{\boldsymbol{\tau}_d}_{\text{disturbance}} \tag{5}$$

As indicated in (5), the element $\mathbf{H}$ is very complicated with mainly three parts: the remaining manipulator dynamics,

the motor dynamics and the unknown lumped disturbance. Therefore, it will be extremely difficult to obtain $\mathbf{H}$ with the traditional methods.

B. PROBLEM DESCRIPTION

The objective of this paper is to design a proper model-free controller $\boldsymbol{\tau}_m$ such that high performance tracking of the desired trajectory $\mathbf{q}_\mathrm{d}$ can be ensured. To realize this objecttive, following assumptions will be required [45]:

Property 1: The inertial matrix $\mathbf{M}(\mathbf{q})$ given in (2)is positive definite symmetrical and bounded such that

$$M_1 \leq \|\mathbf{M}(\mathbf{q})\| \leq M_2 \tag{6}$$

where M_1 and M_2 are two positive constants known beforehand.

Assumption 1: The desired trajectory $\mathbf{q}_\mathrm{d}$ is smooth, *i.e.* $\dot{\mathbf{q}}_d$, $\ddot{\mathbf{q}}_d$ exist and bounded.

Assumption 2: The joint velocity and acceleration signals are bounded.

III. CNFTSM CONTROL DESIGN WITH TDE AND STA

A novel CNFTSM control is designed using TDE and modified STA scheme. The TDE technique is applied as a basic framework of the overall controller to obtain the fascinating model-free feature; while the CNFTSM control with modified STA scheme is used to achieve high tracking precision and good dynamical performance in both the reaching and sliding mode phases.

A. TIME-DELAY ESTIMATION

As demonstrated above, traditional methods may be too complicated or time-consuming to obtain $\mathbf{H}$. Thus, the socalled TDE technique is applied here as

$$\hat{\mathbf{H}}(t) \cong \mathbf{H}(t-L) = \boldsymbol{\tau}_m(t-L) - \bar{\mathbf{M}}\ddot{q}(t-L) \tag{7}$$

It can be observed clearly from (7) that no system dynamics information is required to perform TDE and therefore the attractive model-free nature is ensured. Moreover, the past control torque $\boldsymbol{\tau}_m(t-L)$ and acceleration $\ddot{\mathbf{q}}(t-L)$ are the only required signals to apply TDE. For $\boldsymbol{\tau}_m(t-L)$, it can be easily obtained using the time-delay value of $\boldsymbol{\tau}_m$. For $\ddot{\mathbf{q}}(t-L)$, it is usually obtained through numerical differentiation in TDE-based control schemes as [42]

$$\begin{cases} \ddot{q}_i(t-L) = (q_i(t) - 2q_i(t-L) \\ \qquad\qquad +q_i(t-2L))/L^2, & t > T \\ \ddot{q}_i(t-L) = 0, & t \leq T \end{cases} \tag{8}$$

where $T \geq 2L$ is applied to ease the potential drastic fluctuation in the initial period $t < 2L$. Usually, the acceleration sensors will not be equipped in the manipulators, therefore calculation (8) and its corresponding original version $\ddot{q}_i(t-L) = (q_i(t) - 2q_i(t-L) + q_i(t-2L))/L^2$, $t \geq 0$ had been widely used in TDE-based controllers [2], [38]–[42]. It is also obvious that (8) will obviously amplify the effect of the measurement noise, which, however, can be effectively suppressed with relative smaller control parameter $\bar{\mathbf{M}}$ or low-pass filers [38]–[42].

B. EXISTING TDE-BASED SM CONTROL WITH STA

Define the tracking error as $\mathbf{e} = \mathbf{q}_\mathrm{d} - \mathbf{q}$ with $\mathbf{q}_\mathrm{d}$ as the desired trajectory. Then, the recently proposed TDE-based SM control with STA can be expressed as [45]

$$\bar{\boldsymbol{\tau}}_m = \bar{\mathbf{M}}\left(\ddot{\mathbf{q}}_d + \boldsymbol{\eta}_1\dot{\mathbf{e}} + \mathbf{k}_1\mathbf{sig}(\bar{\mathbf{s}})^{0.5} + \mathbf{k}_3\int_0^t \mathbf{sgn}(\bar{\mathbf{s}})dt\right) + \bar{\boldsymbol{\tau}}_m(t-L) - \bar{\mathbf{M}}\ddot{\mathbf{q}}(t-L) \tag{9}$$

with SM and STA scheme defined as (10) and (11)

$$\bar{\mathbf{s}} = \dot{\mathbf{e}} + \boldsymbol{\eta}_1\mathbf{e} \tag{10}$$

$$\begin{aligned} \dot{\bar{\mathbf{s}}} &= -\mathbf{k}_1\mathbf{sig}(\bar{\mathbf{s}})^{0.5} + \boldsymbol{\vartheta} \\ \dot{\boldsymbol{\vartheta}} &= -\mathbf{k}_3\mathbf{sgn}(\bar{\mathbf{s}}) \end{aligned} \tag{11}$$

where the notations $\bar{\boldsymbol{\tau}}_m, \bar{\mathbf{s}}$ are used to distinguish themselves from the ones we will design latter, meanwhile $\boldsymbol{\eta}_1$, $\mathbf{k}_1$, $\mathbf{k}_3$ are positive diagonal parameter matrices. It should be noted that all the parameters used in (9)-(11) are the same with the control scheme we are going to present. More details concerning above control scheme, please refer to [45].

It can be observed clearly that the existing control (9)uses traditional linear SM manifold and standard STA scheme. However, it had been widely demonstrated that TSM control can provide with better comprehensive control performance than the traditional linear SM control [24], [38]. On the other hand, the standard STA scheme can also be further improved to achieve better comprehensive performance in the reaching phase. To effectively solve above issues, we will present a novel TDE-based CNFTSM control with modified STA scheme in the next subsection.

C. TDE-BASED CNFTSM CONTROL DESIGN WITH MODIFIED STA

To ensure fast convergence and singularity-free dynamical performance, the following NFTSM manifold is designed

$$\mathbf{s} = \dot{\mathbf{e}} + \boldsymbol{\eta}_1\mathbf{e} + \boldsymbol{\eta}_2\boldsymbol{\rho}(\mathbf{e}) \tag{12}$$

where $\boldsymbol{\eta}_1$, $\boldsymbol{\eta}_2$ are the diagonal parameter matrices, while the ith element of $\boldsymbol{\rho}(\mathbf{e})$ is designed as

$$\rho(e)_i = \begin{cases} sig(e_i)^{\alpha_i}, & \bar{s}_i = 0 \vee s_i \neq 0, \ |e_i| \geq \mu_i \\ l_{1i}e_i + l_{2i}\mathrm{sgn}(e_i)e_i^2, & \bar{s}_i \neq 0, \ |e_i| \leq \mu_i \end{cases} \tag{13}$$

where $\bar{s}_i = \dot{e}_i + \eta_{1i}e_i + \eta_{2i}sig(e_i)^{\alpha_i}$, $0.5 < \alpha_i < 1$, $\mu_i > 0$, $i = 1 \sim n$ and $sig(e_i)^{\alpha_i} = |e_i|^{\alpha_i}\mathrm{sgn}(e_i)$ is utilized for simplicity with $\mathrm{sgn}(e_i)$ defined as

$$\mathrm{sgn}(e_i) = \begin{cases} 1, & \text{if } e_i > 0 \\ 0, & \text{if } e_i = 0 \\ -1, & \text{if } e_i < 0 \end{cases} \tag{14}$$

Meanwhile, the parameters l_{1i} and l_{2i} are calculated as

$$l_{1i} = (2-\alpha_i)\,\mu_i^{\alpha_i-1} \tag{15}$$

$$l_{2i} = (\alpha_i-1)\,\mu_i^{\alpha_i-2} \tag{16}$$

The designed NFTSM manifold with above parameters (15) and (16) is singularity-free and continuous, while the first-order derivative of $\boldsymbol{\rho}\,(\mathbf{e})$ is calculated as

$$\dot{\rho}\,(e)_i = \begin{cases} \alpha_i\,|e_i|^{\alpha_{1i}-1}\,\dot{e}_i, & \bar{s}_i = 0 \vee \bar{s}_i \neq 0,\ \ |e_i| \geq \mu_i \\ l_{1i}\dot{e}_i + 2l_{2i}\,|e_i|\,\dot{e}_i, & \bar{s}_i \neq 0,\ \ |e_i| \leq \mu_i \end{cases} \tag{17}$$

It can be clearly observed from (17) that the singularity problem has been successfully eased, while the NFTSM still remains continuous.

To ensure good comprehensive dynamical performance in the reaching phase under complex lumped disturbance, the modified STA scheme is used here as

$$\begin{aligned} \dot{\mathbf{s}} &= -\mathbf{k}_1\mathbf{sig}\,(\mathbf{s})^{0.5} - \mathbf{k}_2\mathbf{s} + \boldsymbol{\vartheta} \\ \dot{\boldsymbol{\vartheta}} &= -\mathbf{k}_3\mathbf{sgn}\,(\mathbf{s}) - \mathbf{k}_4\mathbf{s} \end{aligned} \tag{18}$$

where $\mathbf{k}_1$, $\mathbf{k}_2$, $\mathbf{k}_3$, $\mathbf{k}_4$ are diagonal parameter matrices which will be determined later, and $\mathbf{sig(s)}^{0.5} = [\mathrm{sig(s_1)}^{0.5}, \ldots, \mathrm{sig(s_n)}^{0.5}]^{\mathrm{T}}$, $i = 1 \sim n$.

Then, the proposed CNFTSM control with modified STA scheme is given as

$$\begin{aligned} \boldsymbol{\tau}_m &= \bar{\mathbf{M}}\mathbf{u} + \hat{\mathbf{H}} \\ \mathbf{u} &= \ddot{\mathbf{q}}_d + \boldsymbol{\eta}_1\dot{\mathbf{e}} + \boldsymbol{\eta}_2\dot{\boldsymbol{\rho}}\,(\mathbf{e}) + \mathbf{k}_1\mathbf{sig}\,(\mathbf{s})^{0.5} \\ &\quad + \mathbf{k}_2\mathbf{s} + \mathbf{k}_3\int_0^t \mathbf{sgn}\,(\mathbf{s})\,dt + \mathbf{k}_4\int_0^t \mathbf{s}\,dt \end{aligned} \tag{19}$$

where $\hat{\mathbf{H}}$ stands for estimation of the lumped disturbance $\mathbf{H}$ described in (5).

To obtain $\hat{\mathbf{H}}$ in a simple matter, the TDE technique is applied with (7). Fianlly, our proposed method is given as

$$\begin{aligned} \boldsymbol{\tau}_m = \bar{\mathbf{M}}\Big(&\ddot{\mathbf{q}}_d + \boldsymbol{\eta}_1\dot{\mathbf{e}} + \boldsymbol{\eta}_2\dot{\boldsymbol{\rho}}\,(\mathbf{e}) + \mathbf{k}_1\mathbf{sig}\,(\mathbf{s})^{0.5} + \mathbf{k}_2\mathbf{s}\,(t) \\ &+ \mathbf{k}_3\int_0^t \mathbf{sgn}\,(\mathbf{s})\,dt + \mathbf{k}_4\int_0^t \mathbf{s}\,dt\Big) + \boldsymbol{\tau}_m\,(t-L) \\ &- \bar{\mathbf{M}}\ddot{\mathbf{q}}\,(t-L) \end{aligned} \tag{20}$$

where the diagonal parameter matrices$\mathbf{k}_1$, $\mathbf{k}_2$, $\mathbf{k}_3$, $\mathbf{k}_4$ should satisfy following condition:

$$\begin{aligned} &k_{1i} > 2\delta_{1i}^{0.5}, \quad k_{2i} > (2\delta_{2i})^{0.5}\Big/2,\ k_{3i} > \delta_{1i}, \\ &k_{4i} > \frac{k_{1i}^3\,(2k_{2i}-\delta_{2i}) + \left(5k_{2i}^2 + 2\delta_{2i}\right)p_{1i}}{2p_{1i} - k_{1i}^3} \end{aligned} \tag{21}$$

with p_{1i} given as

$$p_{1i} = k_{1i}\left(\frac{1}{4}k_{1i}^2 - \delta_{1i}\right) + \frac{1}{2}k_{1i}\left(2k_{3i} + \frac{1}{2}k_{1i}^2\right) \tag{22}$$

Corresponding stability analysis and selection of $\mathbf{k}_1$, $\mathbf{k}_2$, $\mathbf{k}_3$, $\mathbf{k}_4$ will be demonstrated in next section.

Comparing the proposed control scheme (20) with the existing one (9), we can see that the NFTSM error dynamics and modified STA scheme are used, which in turn will bring in faster convergence and higher control accuracy. On the other hand, our newly developed TDE-based CNFTSM control with modified STA scheme also brings in extra difficulty to use compared with the existing method (9). To adopt our newly proposed method, more control parameters must be tuned properly through simulations or experiments. Therefore, our proposed method should be applied when the control performance requirement is relative rigorous; otherwise, the existing one (9) can be used for simplicity.

Remark 1: Compared with the traditional TSM control using discontinuous term sgn(**s**), the proposed TDE-based CNFTSM control (20) utilizes no discontinuous element thanks to the application of modified STA scheme. Thus, the proposed control is *continuous* and *chatter-free*. On the other hand, the proposed control, as a typical TSM control scheme, can still remain the advantages of TSM control, such as fast convergence and high control accuracy.

Remark 2: Although the proposed control (20) is designed particularly for the cable-driven manipulators in this paper, it can also be used in other systems, such as extremity exoskeleton [8], [44], biaxial gantry [47], [48], generalized Lorenz system [49], switched nonlinear systems [50], [51]. In the further, we will try to extend the proposed control scheme to the descriptor systems [52]–[55].

IV. STABILITY ANALYSIS

Stability of the closed-loop control system with NFTSM and modified STA dynamics is briefly proved here using similar analysis procedure from [55]–[57]. For simplicity, we will take the *i*th-DOF to analyze.

Substituting the proposed control (19) into (4) gives

$$\begin{aligned} \dot{s}_i &= -k_{1i}\mathrm{sig}\,(s_i)^{0.5} - k_{2i}s_i + \vartheta_i \\ \dot{\vartheta}_i &= -k_{3i}\mathrm{sgn}\,(s_i) - k_{4i}s_i + \dot{\varepsilon}_i \end{aligned} \tag{23}$$

where $\varepsilon_i = -\bar{M}_{ii}\left(\hat{H}_i - H_i\right)$ is the TDE error caused by the application of TDE technique.

Define a new vector $\boldsymbol{\varsigma} = \left[sig\,(s_i)^{0.5}, s_i, \vartheta_i\right]^T$ with initial value given by $\boldsymbol{\varsigma}\,(t_0)$. It is obvious that when $\boldsymbol{\varsigma}$ converges to zero, s_i and ϑ_i will converge to zero accordingly.

Then, select a Lyapunov function as

$$\begin{aligned} V\,(\boldsymbol{\varsigma}) = &2k_{3i}\,|s_i| + k_{4i}s_i^2 + 0.5\boldsymbol{\vartheta}_i^2 \\ &+ 0.5\left(k_{1i}sig\,(s_i)^{0.5} + k_{2i}s_i - \boldsymbol{\vartheta}_i\right)^2 \end{aligned} \tag{24}$$

Re-express (24) in a compact form as

$$V\,(\boldsymbol{\varsigma}) = \boldsymbol{\varsigma}^T\boldsymbol{\Omega}\boldsymbol{\varsigma} \tag{25}$$

with $\boldsymbol{\Omega} = \boldsymbol{\Omega}^T$ defined as

$$\boldsymbol{\Omega} = \frac{1}{2}\begin{bmatrix} \left(4k_{3i} + k_{1i}^2\right) & k_{1i}k_{2i} & -k_{1i} \\ k_{1i}k_{2i} & \left(2k_{4i} + k_{2i}^2\right) & -k_{2i} \\ -k_{1i} & -k_{2i} & 2 \end{bmatrix} \tag{26}$$

Remark 3 [56], [57]: The selected Lyapunov function V is continuous but not locally Lipschitz noting that V is

differentiable everywhere except at $s_i = 0$. Thus, the well-known Lyapunov's second method will be no longer valid here. However, as demonstrated in [57], the convergence properties can still be effectively proved by means of Zubov's theorem [58] which only requires the Lyapunov function to be continuous. Meanwhile, the arguments given in [58] and [59] were used where the derivative of V does not exist. For detailed information concerning this issue, please refer to [57].

Then, following inequality holds

$$\lambda_{\min}\{\mathbf{\Omega}\}\|\boldsymbol{\varsigma}\|_2^2 \le V(\boldsymbol{\varsigma}) \le \lambda_{\max}\{\mathbf{\Omega}\}\|\boldsymbol{\varsigma}\|_2^2 \tag{27}$$

where $\|\boldsymbol{\varsigma}\|_2^2 = |s_i| + s_i^2 + \vartheta_i^2$ stands for the Euclidean norm of $\boldsymbol{\varsigma}$, and $\lambda_{\min}\{\mathbf{\Omega}\}, \lambda_{\max}\{\mathbf{\Omega}\}$ stand for the minimum and maximum eigenvalues of the matrix Ω, respectively.

The temporal derivative of $V(\boldsymbol{\varsigma})$ can be expressed as

$$\dot{V}(\boldsymbol{\varsigma}) = -\frac{1}{|s_i|^{0.5}}\boldsymbol{\varsigma}^T\mathbf{\Omega}_1\boldsymbol{\varsigma} - \boldsymbol{\varsigma}^T\mathbf{\Omega}_2\boldsymbol{\varsigma} + \boldsymbol{\psi}_1^T\boldsymbol{\varsigma} \tag{28}$$

where

$$\mathbf{\Omega}_1 = \mathbf{\Omega}_1^T = \frac{k_{1i}}{2}\begin{bmatrix}(2k_{3i}+k_{1i}^2) & 0 & -k_{1i}\\ 0 & (2k_{4i}+5k_{2i}^2) & -3k_{2i}\\ -k_{1i} & -3k_{2i} & 1\end{bmatrix}$$

$$\mathbf{\Omega}_2 = \mathbf{\Omega}_2^T = k_{2i}\begin{bmatrix}(k_{3i}+2k_{1i}^2) & 0 & 0\\ 0 & (k_{4i}+k_{2i}^2) & -k_{2i}\\ 0 & -k_{2i} & 1\end{bmatrix}$$

$$\boldsymbol{\psi}_1^T = \begin{bmatrix}-k_{1i}\dot{\varepsilon} & -k_{2i}\dot{\varepsilon} & 0\end{bmatrix}$$

Considering the time derivative of TDE error is bounded as $|\dot{\varepsilon}_i| < \delta_{1i} + \delta_{2i}|s_i|, \delta_{1i} > 0, \delta_{2i} > 0$ (Detailed proof can be found in [45]), we have

$$\boldsymbol{\psi}_1^T\boldsymbol{\varsigma} \le \frac{1}{|s_i|^{0.5}}\boldsymbol{\varsigma}^T\mathbf{\Delta}_1\boldsymbol{\varsigma} + \boldsymbol{\varsigma}^T\mathbf{\Delta}_2\boldsymbol{\varsigma} \tag{29}$$

where

$$\mathbf{\Delta}_1 = \begin{bmatrix}k_{1i}\delta_{1i} & 0 & 0\\ 0 & k_{1i}\delta_{2i} & 0\\ 0 & 0 & 0\end{bmatrix}, \quad \mathbf{\Delta}_2 = \begin{bmatrix}k_{2i}\delta_{1i} & 0 & 0\\ 0 & k_{2i}\delta_{2i} & 0\\ 0 & 0 & 0\end{bmatrix}.$$

Combining (28) and (29) gives

$$\dot{V}(\boldsymbol{\varsigma}) \le -\frac{1}{|s_i|^{0.5}}\boldsymbol{\varsigma}^T(\mathbf{\Omega}_1 - \mathbf{\Delta}_1)\boldsymbol{\varsigma} - \boldsymbol{\varsigma}^T(\mathbf{\Omega}_2 - \mathbf{\Delta}_2)\boldsymbol{\varsigma} \tag{30}$$

The $\dot{V}(\boldsymbol{\varsigma})$ will be negative definite if $(\mathbf{\Omega}_1 - \mathbf{\Delta}_1) > 0$ and $(\mathbf{\Omega}_2 - \mathbf{\Delta}_2) > 0$ are satisfied (sufficient condition), which gives the condition (21), (22). It can be observed clearly that it is always possible to choose positive gains $k_{1i}, k_{2i}, k_{3i}, k_{4i}$, $i = 1 \sim n$ such that the condition (21) is fulfilled for every $\delta_{1i}, \delta_{2i}, i = 1 \sim n$.

Using (30), we have

$$\dot{V}(\boldsymbol{\varsigma}) \le -\frac{1}{|s_i|^{0.5}}\lambda_{\min}\{\mathbf{\Omega}_1 - \mathbf{\Delta}_1\}\|\boldsymbol{\varsigma}\|_2^2 - \lambda_{\min}\{\mathbf{\Omega}_2 - \mathbf{\Delta}_2\}\|\boldsymbol{\varsigma}\|_2^2 \tag{31}$$

Substituting (27) and $|s_i|^{0.5} \le \|\boldsymbol{\varsigma}\|_2 \le V^{0.5}(\boldsymbol{\varsigma})/\lambda_{\min}^{0.5}\{\mathbf{\Omega}\}$ into (31) yields

$$\dot{V}(\boldsymbol{\varsigma}) \le -\rho_1 V^{0.5}(\boldsymbol{\varsigma}) - \rho_2 V(\boldsymbol{\varsigma}) \le -\rho_1 V^{0.5}(\boldsymbol{\varsigma}) \tag{32}$$

where

$$\rho_1 = \frac{\lambda_{\min}^{0.5}\{\mathbf{\Omega}\}\lambda_{\min}\{\mathbf{\Omega}_1 - \mathbf{\Delta}_1\}}{\lambda_{\max}\{\mathbf{\Omega}\}}, \quad \rho_2 = \frac{\lambda_{\min}\{\mathbf{\Omega}_2 - \mathbf{\Delta}_2\}}{\lambda_{\max}\{\mathbf{\Omega}\}} \tag{33}$$

According to (32), $V(\boldsymbol{\varsigma})$ and $\boldsymbol{\varsigma}$ will converge to zero in finite time at most after $T_1 = 2V^{0.5}(\boldsymbol{\varsigma}(t_0))/\rho_1$. Thus, the NFTSM variable s_i will converge to zero within T_1. Then, according to the definition of NFTSM manifold (12)-(13), we have $\dot{e}_i + \eta_{1i}e_i + \eta_{2i}sig(e_i)^{\alpha_i} = 0$. Finally, it can be easily derived that the tracking error e_i will converge to zero in finite time.

V. SIMULATION STUDIES

A. SIMULATION SETUP

Simulation studies were performed to demonstrate the effectiveness and superiorities of our newly proposed method over the existing methods. The dynamics model for (2) are directly taken from [38] except for $\boldsymbol{\tau}_d$ which will be given later. Other parameters are selected as $\mathbf{J}$ = [0.5, 0; 0, 0.2] Kg·m^2, $\mathbf{D}_m$ = [0.1, 0; 0, 0.02] N·m·s/rad, $\mathbf{D}_s$ = [50, 0; 0, 40] N·m·s/rad, $\mathbf{K}_s$ = [2, 0; 0, 1] 10^4 N·m/rad. The desired trajectory $\mathbf{q}_d$ is generated using fifth-order polynomial method with the path segments given in Table 1, which is also taken from [38].

TABLE 1. Path segments for the generation of desired trajectory.

t (s)	0.0	3.0	7.0	11.0	15.0
q_1 (°)	0.0	30	-30	30	0.0
q_2 (°)	0.0	30	-30	30	0.0

Three control methods including our newly proposed one were simulated and analyzed in this section. The first one is our newly proposed one; the second one, referred as Controller 2, is given in (9)-(11) which combines the traditional SM control with TDE and STA schemes; the third one, referred as Controller 3, is taken from [42] as

$$\begin{aligned}\vec{\boldsymbol{\tau}}_m &= \bar{\mathbf{M}}\mathbf{u} + \hat{\mathbf{H}}\\ \vec{\mathbf{u}} &= \ddot{\mathbf{q}}_d + \mathbf{c}_2^{-1}\boldsymbol{\gamma}^{-1}\Big[\Big(1 + \mathbf{c}_1\boldsymbol{\psi}\,|\mathbf{e}|^{\boldsymbol{\psi}-1}\Big)\mathbf{sig}(\dot{\mathbf{e}})^{2-\boldsymbol{\gamma}}\\ &\qquad + \mathbf{K}_1\mathbf{sig}(\vec{\mathbf{s}})^{\beta} + \mathbf{K}_2\vec{\mathbf{s}}\Big]\end{aligned} \tag{34}$$

with NFTSM manifold defined as

$$\vec{\mathbf{s}} = \mathbf{e} + \mathbf{c}_1\mathbf{sig}(\mathbf{e})^{\boldsymbol{\psi}} + \mathbf{c}_2\mathbf{sig}(\dot{\mathbf{e}})^{\boldsymbol{\gamma}} \tag{35}$$

where $\vec{\boldsymbol{\tau}}_m, \vec{\mathbf{u}}, \vec{\mathbf{s}}$ are used to distinguish themselves from the ones given above. Meanwhile, $c_{1i}, c_{2i}, \psi_i, \gamma_i$ are positive constant parameters and the condition $1 < \gamma_i < 2, \psi_i > \gamma_i$ must be fulfilled. Compared with our newly proposed method, Controller 3 uses the widely adopted fast-TSM-type reaching law which can provide with good control performance as well as effective suppression of the chattering problem.

B. SIMULATION RESULTS

The control parameters for our newly proposed controller are selected as $\eta_1 = \eta_2 = \text{diag}(1, 1)$, $\alpha = \text{diag}(0.8, 0.8)$, $\mu = \text{diag}(0.1, 0.1)$, $\mathbf{k}_1 = \text{diag}(4, 4)$, $\mathbf{k}_2 = \text{diag}(0.1, 0.1)$, $\mathbf{k}_3 = \text{diag}(1, 1)$, $\mathbf{k}_4 = \text{diag}(2, 2)$, $\bar{\mathbf{M}} = \text{diag}(0.12, 0.12)$, $L = 1$ms, and the simulation sampling period is set to 1ms. For comparison fairness, the parameters for Controller 2 are selected exactly the same as ours. The parameters for Controller 3 are selected as $\mathbf{c}_1 = \mathbf{c}_2 = \text{diag}(1, 1)$, $\psi = \text{diag}(1.3, 1.3)$, $\gamma = \text{diag}(1.25, 1.25)$, $\mathbf{K}_1 = diag(4, 4)$, $\mathbf{K}_2 = \text{diag}(1, 1)$, $\beta = \text{diag}(0.5, 0.5)$. A time-varying uncertainties $\tau_d = \sin(\pi t)$ N·m is added to verify the robustness. Note that τ_d is obvious faster than the desired trajectory $\mathbf{q}_d$. Corresponding results are given in Fig. 1-6.

As shown in Fig. 1, all three controllers can provide with satisfactory control performance under unknown lumped disturbance, which effectively proves the validity of TDE technique (7), existing methods (34) and our newly proposed one (19). On the other hand, our proposed method (19) using NFTSM manifold (12)(13) and modified STA (18) can still guarantee the best control performance among all three controllers as indicated in Fig. 2 and Fig. 4-6. Taking Fig. 4-6 to analyze, we can see that our method provides with the fastest

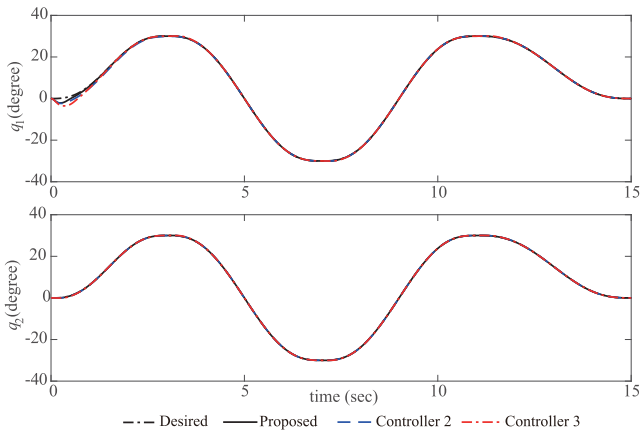

FIGURE 1. Simulation results: trajectory tracking control performance of joint 1 and 2.

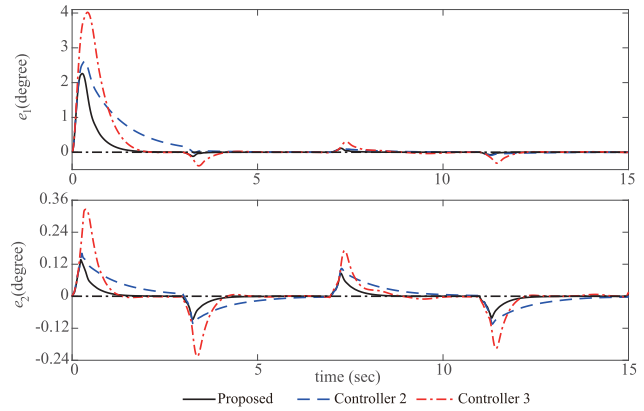

FIGURE 2. Simulation results: tracking errors of joint 1 and 2.

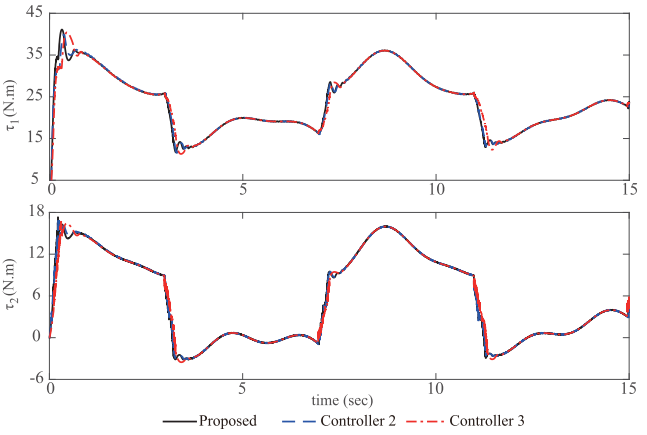

FIGURE 3. Simulation results: control inputs of joint 1 and 2.

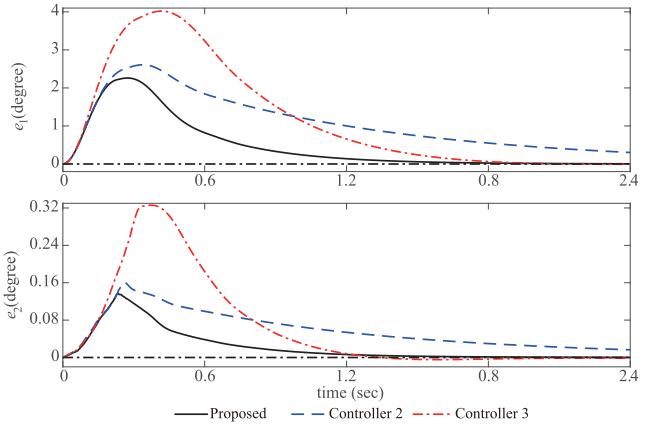

FIGURE 4. Simulation results: tracking errors of joint 1 and 2 in initial phase.

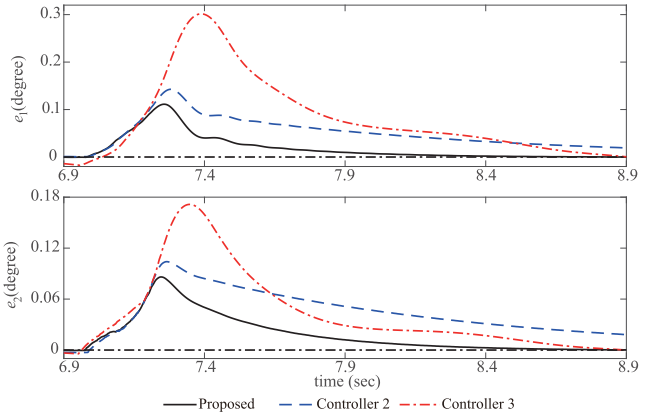

FIGURE 5. Simulation results: tracking errors of joint 1 and 2 in peak phase.

convergence, while Controller 2 shows relative the worst. For tracking precision, our method shows the best; meanwhile Controller 3 gives relative the worst.

Thanks to the NFTSM (12)(13) and modified STA (18) schemes, fast convergence and high accuracy and good robustness have been effectively achieved.

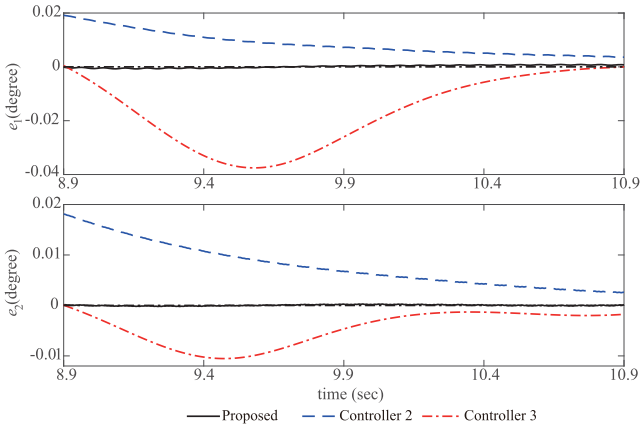

FIGURE 6. Simulation results: tracking errors of joint 1 and 2 in steady phase.

In general, all three TDE-based robust controls can provide with good tracking of the desired trajectory, while our newly proposed one can guarantee relative the best comprehensive control performance. Fast convergence, high tracking precision and strong robustness against time-varying disturbance have been clearly observed with our proposed method.

VI. EXPERIMENTAL STUDIES

To further demonstrate the effectiveness and superiorities of our newly proposed TDE-based CNFTSM control with modified STA scheme in practical applications, two comparative experiments had been performed using a cable-driven manipulator Polaris-I which was developed in our laboratory as shown in Fig. 7. In first experiment, Polaris-I was commanded to track a combined sinusoidal signal without payload. In second experiment, a payload of 0.5Kg was added to Polaris-I to verify the robustness of our newly proposed method.

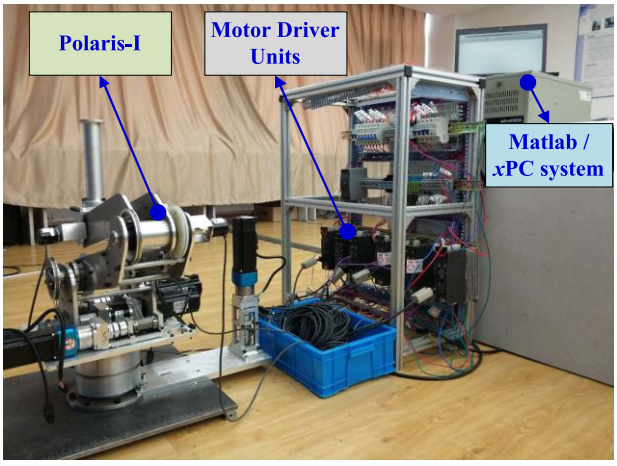

FIGURE 7. Experimental setup: Polaris-I and its control system.

A. EXPERIMENTAL SETUP

The motors used in Polaris-I are Delta ECMA-CA0604SS which have rated speed of 3000rpm and rated torque of 1.27 N·m, respectively. As shown in Fig. 7, the motors are installed in the base and drive the joints through cables. This kind of design can effectively reduce the moving mass and bring in good flexibility and cooperation safety. The motor drivers are ASD-A2-042-L, meanwhile both cable and planetary reducers are utilized which have reduction ratio of 1:3.3 and 1:10. The used encoders E6B2-CWZ1X 2000P/R have a resolution of 0.045 degree. Finally, the control algorithms are executed using the x PC system with a NI PCI-6229 board. The sampling frequency is set to 1kHz in following experiments.

All three TDE-based controls simulated in previous section were experimented here. The control parameters for our newly proposed method are selected as $\boldsymbol{\eta}_1 = \text{diag}(3, 3)$, $\boldsymbol{\eta}_2 = \text{diag}(2, 2)$ $\boldsymbol{\alpha} = \text{diag}(0.8, 0.8)$, $\mu = \text{diag}(0.2, 0.1)$, $\mathbf{k}_1 = \text{diag}(1.2, 1.2)$, $\mathbf{k}_2 = \text{diag}(0.35, 0.35)$, $\mathbf{k}_3 = \text{diag}(0.15, 0.2)$, $\mathbf{k}_4 = \text{diag}(1.5, 1.5)$, $\bar{\mathbf{M}} = \text{diag}(0.011, 0.012)$, $L = 2$ms, and the experimental sampling period is set to 1ms. For comparison fairness, the parameters for Controller 2 are selected exactly the same as ours. Meanwhile, the parameters for Controller 3 are selected as $\mathbf{c}_1 = \text{diag}(1.7, 1.7)$, $\mathbf{c}_2 = \text{diag}(0.5, 0.5)$, $\boldsymbol{\psi} = \text{diag}(1.8, 1.8)$, $\boldsymbol{\gamma} = \text{diag}(1.25, 1.25)$, $\mathbf{K}_1 = \text{diag}(4, 4)$, $\mathbf{K}_2 = \text{diag}(1, 1)$, $\beta = 0.5$.

B. EXPERIMENTAL RESULTS

1) EXPERIMENT ONE

In this experiment, Polaris-I was commanded to track a combined sinusoidal signal without payload. Corresponding results are given in Fig. 8-11. To accurately describe the control performance, the root-mean-square error (RMSE) and Maximum error (MAE) are calculated using the steady tracking data from 20s to 40s. Corresponding results are given in Table 2.

As indicated in Fig. 8-11, all three control schemes can ensure good tracking of the desired trajectory, which efficiently demonstrate the effectiveness of the TDE technique, the existing CNFTSM control, SM control with STA and our newly proposed method. Moreover, there are three obvious tracking error peaks in the overall control process, which

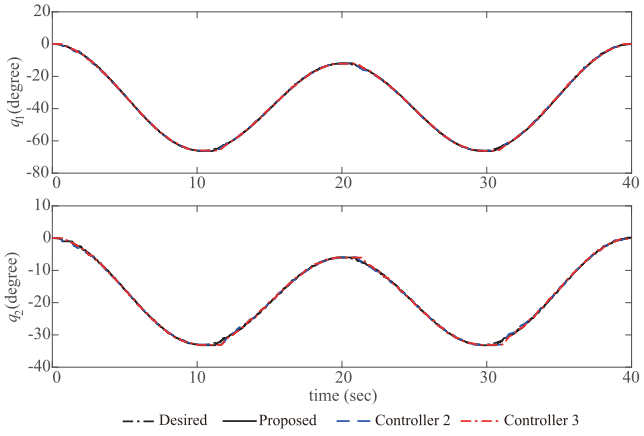

FIGURE 8. Experiment one: trajectory tracking control performance of joint 1 and 2.

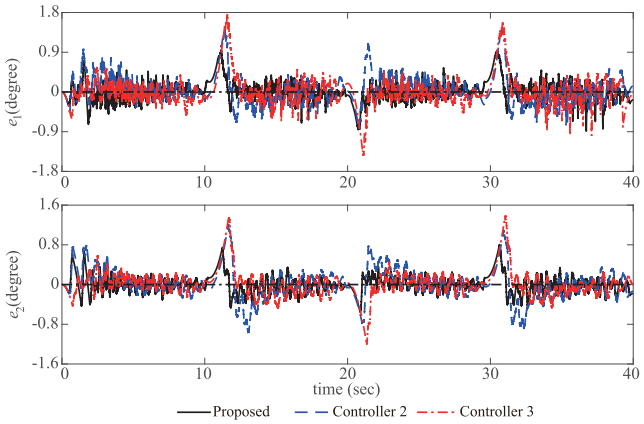

FIGURE 9. Experiment one: tracking errors of joint 1 and 2.

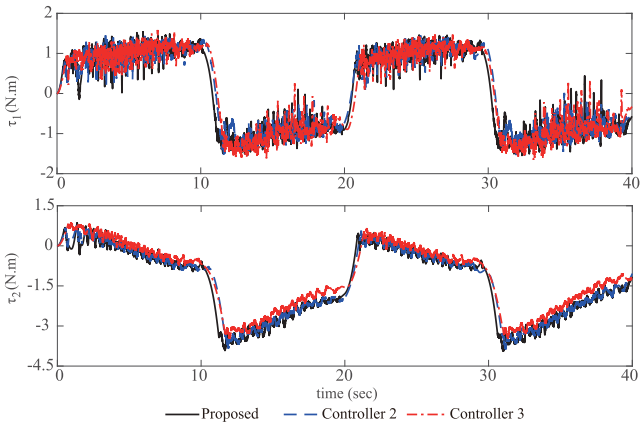

FIGURE 10. Experiment one: control inputs of joint 1 and 2.

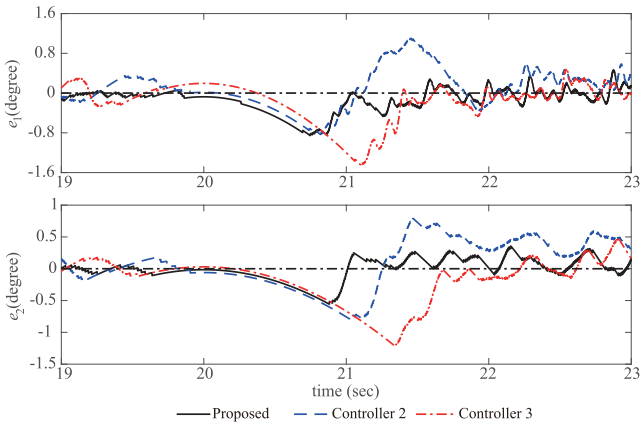

FIGURE 11. Experiment one: tracking errors of joint 1 and 2 in peak phase.

are mainly caused by the frictions. Meanwhile, our newly proposed method can still provide with relative the best control performance among all three methods as show in Fig. 9 and Fig. 11. Higher accuracy and faster convergence had been clearly observed with our proposed method over the other twos. These results have strongly demonstrated the superiorities of our newly proposed method over the existing methods.

TABLE 2. Tracking performance comparisons with three controllers.

(degree)	RMSE (Joint 1/2)	MAE(Joint 1/2)
Proposed	0.25 / 0.18	0.94 / 0.80
Controller 2	0.33 / 0.33	1.27 / 1.05
Controller 3	0.38 / 0.31	1.59 / 1.39

To obtain a precise comparison, we take the RMSE and MAE values in Table 2 to analyze. An indicated in Table 2, all three control schemes can ensure relative good tracking accuracy. Still, our newly proposed one provides with the highest tracking accuracy. For RMSE, our method ensures tracking precisions of 0.25° and 0.18° for joint 1 and 2, which are just 75.8% and 54.5% of those guaranteed by Controller 2 and 65.8% and 58.1% of Controller 3, respectively. For MAE, our method provides with tracking accuracy of 0.94° and 0.80° for joint 1 and 2, which are just 74.0% and 76.2% of Controller 2 and 59.1% and 57.6% of Controller 3, respectively. It can be easily observed from above calculations that our method has brought in obvious control improvement compared with the existing methods. Above analysis is consistent with the simulation results.

2) EXPERIMENT TWO

To verify the robustness of our newly proposed method against uncertainties, a 0.5 Kg payload was added into the Polaris-I. It should be noted that the mass of last two links of Polaris-I are 2.5 Kg and 1.2 Kg, respectively. Therefore, the payload is 20% and 41.7% of the mass of last two links. Corresponding results are given in Fig. 12-14. Also, the RMSE and MAE are calculated using the steady tracking data from 20s to 40s to accurately describe the control performance, which are given in Table 3.

TABLE 3. Tracking performance comparisons without *vs* with payload.

(degree)	RMSE (Joint 1/2)	MAE (Joint 1/2)
no payload	0.25 / 0.18	0.94 / 0.80
with payload	0.23 / 0.20	1.00 / 0.85

As shown in Fig. 12-14, good control performance can still be ensured with our proposed method under 0.5 Kg payload, which effectively demonstrates the robustness of the proposed method. For precise comparison, we take Table 3 to analyze. RMSE decreases 8.0% and increases 11.1% for joint 1 and 2, respectively. Meanwhile, the MAE increases 6.4% and 6.3% for joint 1 and 2, respectively. Considering the links mass and payload, we can clearly see that relative satisfactory robustness has been obtained using our newly proposed method.

Furthermore, comparing Table 2 and 3, we can see that our newly proposed method under 0.5 Kg payload can even provide with higher tracking accuracy than the other twos without payload.

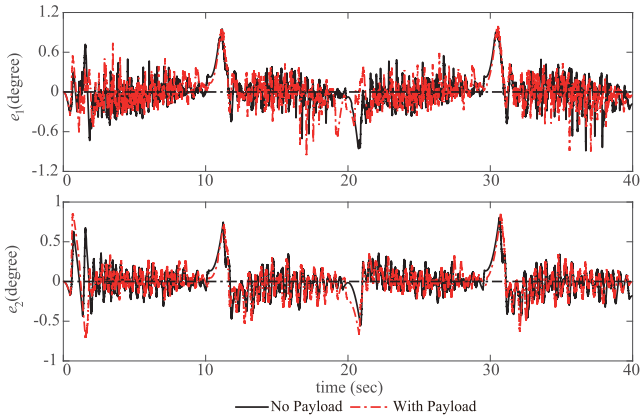

FIGURE 12. Experiment two: tracking errors of joint 1 and 2.

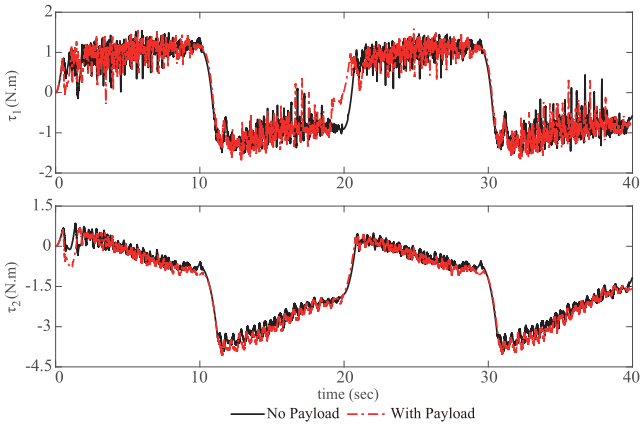

FIGURE 13. Experiment two: control inputs of joint 1 and 2.

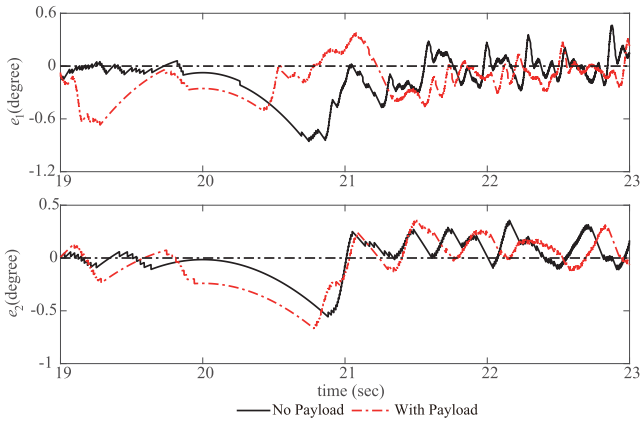

FIGURE 14. Experiment two: tracking errors of joint 1 and 2 in peak phase.

Generally speaking, all three control schemes can ensure satisfactory tracking of the desired trajectory. Meanwhile, the superiorities of our newly proposed method over the existing ones have been experimentally demonstrated.

VII. CONCLUSIONS

In this paper, a novel TDE-based CNFTSM control with modified STA is proposed for the high performance tracking control of cable-driven manipulators under complicated lumped disturbance. The newly proposed method is modelfree and easy to use in complex practical applications thanks to the TDE technique, meanwhile high tracking accuracy and fast dynamical response and strong robustness against lumped disturbance can be effectively ensured benefitting from the designed NFTSM manifold and modified STA schemes. The stability of closed-loop control system with NFTSM and STA dynamics is analyzed. Finally, comparative simulations and experiments were performed. Corresponding results show that our newly proposed TDE-based CNFTSM control with modified STA scheme can provide with faster convergence, higher tracking accuracy and better robustness than the existing methods.

REFERENCES

[1] Y. Wang, L. Gu, B. Chen, and H. Wu, "A new discrete time delay control of hydraulic manipulators," *Proc. Inst. Mech. Eng. I, J. Syst. Control Eng.*, vol. 231, no. 3, pp. 168–177, Mar. 2017.
[2] Y. Wang, L. Gu, Y. Xu, and X. Cao, "Practical tracking control of robot manipulators with continuous fractional-order nonsingular terminal sliding mode," *IEEE Trans. Ind. Electron.*, vol. 63, no. 10, pp. 6194–6204, Oct. 2016.
[3] A. Suarez, G. Heredia, and A. Ollero, "Design of an anthropomorphic, compliant, and lightweight dual arm for aerial manipulation," *IEEE Access*, vol. 6, pp. 29173–29189, May 2018.
[4] D. Banerjee, K. Yu, and G. Aggarwal, "Image rectification software test automation using a robotic arm," *IEEE Access*, vol. 6, pp. 34075–34085, Jun. 2018.
[5] W. T. Townsend, "The effect of transmission design on force-controlled manipulator performance," Ph.D. dissertation, Cambridge Artif. Intell. Lab., Massachusetts Inst. Technol., Cambridge, MA, USA, 1988.
[6] T. Lens and O. von Stryk, "Design and dynamics model of a lightweight series elastic tendon-driven robot arm," in *Proc. IEEE Int. Conf. Robot. Automat.*, Karlsruhe, Germany, May 2013, pp. 4512–4518.
[7] W. B. Lim, S. H. Yeo, and G. Yang, "Optimization of tension distribution for cable-driven manipulators using tension-level index," *IEEE/ASME Trans. Mechatronics*, vol. 19, no. 2, pp. 676–683, Apr. 2014.
[8] Y. Mao, X. Jin, G. G. Dutta, J. P. Scholz, and S. K. Agrawal, "Human movement training with a cable driven ARm EXoskeleton (CAREX)," *IEEE Trans. Neural Syst. Rehabil. Eng.*, vol. 23, no. 1, pp. 84–92, Jan. 2015.
[9] W. Xu, Y. Wang, S. Jiang, J. Yao, and B. Chen, "Kinematic analysis of a newly designed cable-driven manipulator," *Trans. Can. Soc. Mech. Eng.*, vol. 42, no. 2, pp. 125–135, May 2018.
[10] Y. Wang, S. Wang, Q. Wei, M. Tan, C. Zhou, and J. Yu, "Development of an underwater manipulator and its free-floating autonomous operation," *IEEE/ASME Trans. Mechatronics*, vol. 21, no. 2, pp. 815–824, Apr. 2016.
[11] F. Yan, Y. Wang, W. Xu, and B. Chen, "Time delay control of cable-driven manipulators with artificial bee colony algorithm," *Trans. Can. Soc. Mech. Eng.*, vol. 42, no. 2, pp. 177–186, May 2018.
[12] Y. Wang, S. Jiang, B. Chen, and H. Wu, "A new continuous fractional-order nonsingular terminal sliding mode control for cable-driven manipulators," *Adv. Eng. Softw.*, vol. 119, pp. 21–29, May 2018.
[13] Y. Wang, F. Yan, S. Jiang, and B. Chen, "Time delay control of cable-driven manipulators with adaptive fractional-order nonsingular terminal sliding mode," *Adv. Eng. Softw.*, vol. 121, pp. 13–25, Jul. 2018.
[14] A.-C. Huang and Y.-C. Chen, "Adaptive sliding control for single-link flexible-joint robot with mismatched uncertainties," *IEEE Trans. Control Syst. Technol.*, vol. 12, no. 5, pp. 770–775, Sep. 2004.
[15] H. Chaoui, P. Sicard, and W. Gueaieb, "ANN-based adaptive control of robotic manipulators with friction and joint elasticity," *IEEE Trans. Ind. Electron.*, vol. 56, no. 8, pp. 3174–3187, Aug. 2009.
[16] R. Babaghasabha, M. A. Khosravi, and H. D. Taghirad, "Adaptive robust control of fully constrained cable robots: Singular perturbation approach," *Nonlinear Dyn.*, vol. 85, no. 1, pp. 607–620, Jul. 2016.
[17] S. Qian, B. Zi, and H. Ding, "Dynamics and trajectory tracking control of cooperative multiple mobile cranes," *Nonlinear Dyn.*, vol. 83, nos. 1–2, pp. 89–108, Jan. 2016.

[18] Y. Wang, L. Gu, M. Gao, and K. Zhu, "Multivariable output feedback adaptive terminal sliding mode control for underwater vehicles," *Asian J. Contr.*, vol. 18, no. 1, pp. 247–265, Jan. 2016.

[19] W. Qi, G. Zong, and H. R. Karimi, "$\mathcal{L}_\infty$ control for positive delay systems with semi-Markov process and application to a communication network model," *IEEE Trans. Ind. Electron.*, to be published, doi: 10.1109/TIE.2018.2838113.

[20] W. Qi, G. Zong, and H. R. Karimi, "Observer-based adaptive SMC for nonlinear uncertain singular semi-Markov jump systems with applications to DC motor," *IEEE Trans. Circuits Syst. I, Reg. Papers*, vol. 65, no. 9, pp. 2951–2960, Sep. 2018, doi: 10.1109/TCSI.2018.2797257.

[21] H. Sun, L. Hou, G. Zong, and X. Yu, "Fixed-time attitude tracking control for spacecraft with input quantization," *IEEE Trans. Aerosp. Electron. Syst.*, to be published, doi: 10.1109/TAES.2018.2849158.

[22] W. Qi, J. H. Park, J. Cheng, and Y. Kao, "Robust stabilisation for non-linear time-delay semi-Markovian jump systems via sliding mode control," *IET Control Theory Appl.*, vol. 11, no. 10, pp. 1504–1513, 2017.

[23] V. Utkin, J. Guldner, and J. Shi, *Sliding Mode Control in Electro-Mechanical Systems*. Orlando, FL, USA: CRC Press, 1999.

[24] S. Yu, X. Yu, B. Shirinzadeh, and Z. Man, "Continuous finite-time control for robotic manipulators with terminal sliding mode," *Automatica*, vol. 41, no. 11, pp. 1957–1964, Nov. 2005.

[25] W. Deng, J. Yao, and D. Ma, "Robust adaptive precision motion control of hydraulic actuators with valve dead-zone compensation," *ISA Trans.*, vol. 70, pp. 269–278, Sep. 2017.

[26] W. Deng, J. Yao, and D. Wei, "Time-varying input delay compensation for nonlinear systems with additive disturbance: An output feedback approach," *Int. J. Robust Nonlinear Control*, vol. 28, no. 1, pp. 31–52, Jan. 2018.

[27] M. R. Soltanpour and M. H. Khooban, "A particle swarm optimization approach for fuzzy sliding mode control for tracking the robot manipulator," *Nonlinear Dyn.*, vol. 74, nos. 1–2, pp. 467–478, Oct. 2013.

[28] L. Wang, T. Chai, and L. Zhai, "Neural-network-based terminal sliding-mode control of robotic manipulators including actuator dynamics," *IEEE Trans. Ind. Electron.*, vol. 56, no. 9, pp. 3296–3304, Sep. 2009.

[29] H. Joe, M. Kim, and S.-C. Yu, "Second-order sliding-mode controller for autonomous underwater vehicle in the presence of unknown disturbances," *Nonlinear Dyn.*, vol. 78, no. 1, pp. 183–196, Oct. 2014.

[30] J. Yang, J. Su, S. Li, and X. Yu, "High-order mismatched disturbance compensation for motion control systems via a continuous dynamic sliding-mode approach," *IEEE Trans. Ind. Informat.*, vol. 10, no. 1, pp. 604–614, Feb. 2014.

[31] Y. Feng, X. Yu, and F. Han, "High-order terminal sliding-mode observer for parameter estimation of a permanent-magnet synchronous motor," *IEEE Trans. Ind. Electron.*, vol. 60, no. 10, pp. 4272–4280, Oct. 2013.

[32] H. Deng, Q. Li, W. Chen, and G. Zhang, "High-order sliding mode observer based OER control for PEM fuel cell air-feed system," *IEEE Trans. Energy Convers.*, vol. 33, no. 1, pp. 232–244, Mar. 2018.

[33] R. Sadeghi, S. M. Madani, M. R. A. Kashkooli, and S. Ademi, "Super-twisting sliding mode direct power control of a brushless doubly fed induction generator," *IEEE Trans. Ind. Electron.*, vol. 65, no. 11, pp. 9147–9156, Nov. 2018.

[34] R. Seeber, M. Reichhartinger, and M. Horn, "A Lyapunov function for an extended super-twisting algorithm," *IEEE Trans. Autom. Control*, to be published, doi: 10.1109/TAC.2018.2794411.

[35] O. A. Morfin, F. A. Valenzuela, R. R. Betancour, C. E. Castañeda, R. Ruíz-Cruz, and A. Valderrabano-Gonzalez, "Real-time SOSM super-twisting combined with block control for regulating induction motor velocity," *IEEE Access*, vol. 6, pp. 25898–25907, Mar. 2018.

[36] T. C. S. Hsia, "A new technique for robust control of servo systems," *IEEE Trans. Ind. Electron.*, vol. 36, no. 1, pp. 1–7, Feb. 1989.

[37] K. Youcef-Toumi and O. Ito, "A time delay controller for systems with unknown dynamics," *ASME J. Dyn. Syst. Meas. Control*, vol. 112, no. 1, pp. 133–142, 1990.

[38] M. Jin, J. Lee, P. H. Chang, and C. Choi, "Practical nonsingular terminal sliding-mode control of robot manipulators for high-accuracy tracking control," *IEEE Trans. Ind. Electron.*, vol. 56, no. 9, pp. 3593–3601, Sep. 2009.

[39] M. Jin, S. H. Kang, P. H. Chang, and J. Lee, "Robust control of robot manipulators using inclusive and enhanced time delay control," *IEEE/ASME Trans. Mechatronics*, vol. 22, no. 5, pp. 2141–2152, Oct. 2017.

[40] Y. Wang, B. Chen, and H. Wu, "Practical continuous fractional-order nonsingular terminal sliding mode control of underwater hydraulic manipulators with valve deadband compensators," *Proc. Inst. Mech. Eng. M, J. Eng. Maritime Environ.*, to be published, doi: 10.1177/1475090217753900.

[41] Y. Wang, S. Jiang, B. Chen, and H. Wu, "Trajectory tracking control of underwater vehicle-manipulator system using discrete time delay estimation," *IEEE Access*, vol. 5, pp. 7435–7443, Jun. 2017.

[42] Y. Wang, B. Chen, and H. Wu, "Joint space tracking control of underwater vehicle-manipulator systems using continuous nonsingular fast terminal sliding mode," *Proc. Inst. Mech. Eng. M, J. Eng. Maritime Environ.*, to be published, doi: 10.1177/1475090217742241.

[43] X. Zhang, H. Wang, Y. Tian, L. Peyrodie, and X. Wang, "Model-free based neural network control with time-delay estimation for lower extremity exoskeleton," *Neurocomputing*, vol. 272, pp. 178–188, Jan. 2018.

[44] B. Brahmi, M. Saad, C. Ochoa-Luna, M. H. Rahman, and A. Brahmi, "Adaptive tracking control of an exoskeleton robot with uncertain dynamics based on estimated time-delay control," *IEEE/ASME Trans. Mechatronics*, vol. 23, no. 2, pp. 575–585, Apr. 2018.

[45] Y. Kali, M. Saad, K. Benjelloun, and C. Khairallah, "Super-twisting algorithm with time delay estimation for uncertain robot manipulators," *Nonlinear Dyn.*, vol. 93, no. 2, pp. 557–569, Jul. 2018.

[46] M. Jin, J. Lee, and N. G. Tsagarakis, "Model-free robust adaptive control of humanoid robots with flexible joints," *IEEE Trans. Ind. Electron.*, vol. 64, no. 2, pp. 1706–1715, Feb. 2017.

[47] M. Yuan, Z. Chen, B. Yao, and X. Zhu, "Time optimal contouring control of industrial biaxial gantry: A highly efficient analytical solution of trajectory planning," *IEEE/ASME Trans. Mechatronics*, vol. 22, no. 1, pp. 247–257, Feb. 2017.

[48] M. Yuan, Z. Chen, B. Yao, and J. Hu, "An improved on-line trajectory planner with stability-guaranteed critical test curve algorithm for generalized parametric constraints," *IEEE/ASME Trans. Mechatronics*, to be published, doi: 10.1109/TMECH.2018.2862144.

[49] D. Kim, M. Jin, and P. H. Chang, "Control and synchronization of the generalized Lorenz system with mismatched uncertainties using backstepping technique and time-delay estimation," *Int. J. Circuit Theory Appl.*, vol. 45, pp. 1833–1848, Nov. 2017.

[50] D. Zhai, A. Lu, J. Dong, and Q. Zhang, "Switched adaptive fuzzy tracking control for a class of switched nonlinear systems under arbitrary switching," *IEEE Trans. Fuzzy Syst.*, vol. 26, no. 2, pp. 585–597, Apr. 2018.

[51] D. Zhai, A.-Y. Lu, J. Dong, and Q. Zhang, "Adaptive tracking control for a class of switched nonlinear systems under asynchronous switching," *IEEE Trans. Fuzzy Syst.*, vol. 26, no. 3, pp. 1245–1256, Jun. 2018.

[52] J. Li and Q. Zhang, "A linear switching function approach to sliding mode control and observation of descriptor systems," *Automatica*, vol. 95, pp. 112–121, Sep. 2018.

[53] J. Li and Q. Zhang, "Fuzzy reduced-order compensator-based stabilization for interconnected descriptor systems via integral sliding modes," *IEEE Trans. Syst., Man, Cybern., Syst.*, to be published, doi: 10.1109/TSMC.2017.2707499.

[54] J. Li, Q. Zhang, X.-G. Yan, and S. Spurgeon, "Observer-based fuzzy integral sliding mode control for nonlinear descriptor systems," *IEEE Trans. Fuzzy Syst.*, to be published, doi: 10.1109/TFUZZ.2018.2802458.

[55] J. Li, Q. Zhang, X.-G. Yan, and S. K. Spurgeon, "Integral sliding mode control for Markovian jump T–S fuzzy descriptor systems based on the super-twisting algorithm," *IET Control Theory Appl.*, vol. 11, no. 8, pp. 1134–1143, May 2017.

[56] F. Muñoz, I. González-Hernández, S. Salazar, E. S. Espinoza, and R. Lozano, "Second order sliding mode controllers for altitude control of a quadrotor UAS: Real-time implementation in outdoor environments," *Neurocomputing*, vol. 233, pp. 61–71, Apr. 2017.

[57] J. A. Moreno and M. Osorio, "Strict Lyapunov functions for the super-twisting algorithm," *IEEE Trans. Autom. Control*, vol. 57, no. 4, pp. 1035–1040, Apr. 2012.

[58] A. S. Poznyak, "Theorem 20.2," in *Advanced Mathematical Tools for Automatic Control Engineers*, Amsterdam, The Netherlands: Elsevier, 2008, p. 568.

[59] I. Salgado, O. Camacho, C. Yañez, and I. Chairez, "Proportional derivative fuzzy control supplied with second order sliding mode differentiation," *Eng. Appl. Artif. Intell.*, vol. 35, pp. 84–94, Oct. 2014.

[60] J. A. Moreno and M. Osorio, "A Lyapunov approach to second-order sliding mode controllers and observers," in *Proc. 47th IEEE Conf. Decis. Control*, Cancun, Mexico, Dec. 2008, pp. 2856–2861.

YAOYAO WANG (M'17) received the B.S. degree in mechanical engineering from Southeast University, Nanjing, China, in 2011, and the Ph.D. degree in mechanical engineering from Zhejiang University, Hangzhou, China, in 2016.

He is currently a Lecturer with the College of Mechanical and Electrical Engineering, Nanjing University of Aeronautics and Astronautics, Nanjing. His current research interests include robust control and adaptive control of hydraulic manipulators and underwater vehicles and design and control of cable-driven manipulators.

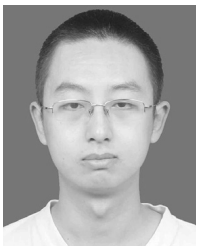

FEI YAN received the B.S. degree in mechanical and electrical engineering from the Jiangsu University of Science and Technology, Zhenjiang, China, in 2015.

He is currently pursuing the Ph.D. degree with the College of Mechanical and Electrical Engineering, Nanjing University of Aeronautics and Astronautics, Nanjing, China. His current research interests include artificial bee colony algorithm and design and control of cable-driven manipulators.

JIAWANG CHEN (M'18) received the B.S. degree in drilling engineering and the Ph.D. degree in geotechnology engineering from the University of Jilin, Changchun, in 2002 and 2007, respectively. From 2007 to 2010, he was a Post-Doctoral Researcher with the State Key Laboratory of Fluid Power and Mechatronic System, Zhejiang University. Since 2010, he has been an Associate Professor with the Department of Ocean Engineering, Zhejiang University. He has authored over 30 articles and over 25 inventions. He holds 12 patents. His research interests include underwater cable deformation monitoring technology, sea land subsidence monitoring technology, and deep-sea instrument development technology such as the pressure corer and pressure core transferring instrument.

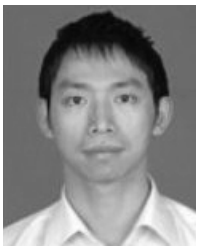

BAI CHEN received the B.S. and Ph.D. degrees in mechanical engineering from Zhejiang University, Hangzhou, China, in 2000 and 2005, respectively.

He is currently a Professor and a Ph.D. Candidate Supervisor with the College of Mechanical and Electrical Engineering, Nanjing University of Aeronautics and Astronautics, Nanjing, China. His current research interests include design and control of surgical robots, cable-driven robots, and sperm-like swimming microrobots.